



1 **Information loss in palaeoecological data from process and**
2 **observer error**

3 Quinn Asena¹, George L. W. Perry¹, and Janet M. Wilmshurst²

4 ¹School of Environment, University of Auckland, 23 Symonds Street, Auckland, New Zealand
5 1010.

6 ²Research Manaaki Whenua – Landcare Research, 76 Gerald Street, Lincoln, New Zealand, 7608

7 Correspondence to: Quinn Asena (qasena@wisc.edu)



8 **Abstract**

9 Palaeoecological data give us insight into how ecosystems have changed in the past, and with the
10 development of new sources of proxy data and statistical methods, they are being used to address
11 questions around the underlying mechanisms of change, such as biotic- and climate-ecosystem
12 interactions. However, inferences from palaeoecological data can be hindered by uncertainties
13 inherent in core-type samples that arise from environmental processes and observer-introduced
14 error. Environmental processes, core extraction methods, sub-sampling strategies, laboratory
15 methods, and data processing can potentially mask ‘true’ signals in the data. The influence of
16 sources of uncertainty on inferences drawn from palaeoecological data are rarely assessed but are
17 critical to the confidence of our conclusions. To address this concern, we use a virtual ecological
18 approach to assess the influences of environmental and observer introduced uncertainty to better
19 understand which of them have the strongest influence on statistical methods applied to the data.
20 Quantifying information loss from uncertainty can be used to inform study design before a
21 project is carried out to increase the likelihood of detecting a given signal of interest and make
22 more robust inferences from statistical analyses of palaeoproxy data. We generate synthetic
23 ‘error-free’ core-type samples of pseudoproxies, on which environmental and observational
24 processes are systematically introduced to impose uncertainties on the simulated pseudoproxies.
25 The influence of three sources of uncertainty (core mixing, sub-sampling, and proxy
26 quantification from sub-samples), are assessed for their individual and combined effects on
27 two statistical methods: Fisher Information and principal curves. Increasing sub-sampling
28 intervals has the most substantial influence on the two statistical methods applied to the
29 pseudoproxy data. When combined, the interaction between increasing sub-sampling interval,
30 and decreasing the number of proxies counted per sub-sample has the strongest influence on
31 Fisher Information and principal curves. Fisher Information and principal curves are not affected
32 in the same way by introducing uncertainty, with principal curves being less influenced by
33 simulated proxy counting and sub-sampling of the core. Virtually assessing uncertainties is a
34 powerful method to better understand the influence that uncertainties introduced at different parts
35 of the analytical process have on conclusions drawn from palaeoecological data.

36



37 **1 Introduction**

38 Palaeoecological data extends the temporal extent over which we can investigate ecosystem
39 change well beyond the observational record (Kosnik and Kowalewski 2016). These long-term
40 records are crucial for understanding ecosystem trajectories and climate-ecosystem interactions,
41 as such dynamics may unfold over centuries or millennia (Jackson 2007). A growing number of
42 proxies and statistical methods are available to address how ecosystems respond to
43 environmental and human pressures through time. Palaeoecologists seek to use these data to go
44 beyond describing past changes in, for example, the relative abundances of species, to uncover
45 underlying mechanisms of change such as biotic interactions and species-environment
46 relationships (Williams, Blois, and Shuman 2011). However, the inferences drawn from
47 palaeoecological data may be hindered or even limited by their uncertainties, such as a paucity of
48 observations over time and space, environmental degradation of samples, and observer-
49 introduced error. Thus, to make robust inferences from palaeoecological data, such uncertainties
50 need to be better understood and quantified.

51 **1.1 Uncertainties in palaeoecological data**

52 Palaeoecological data derived from core-type samples are subject to numerous uncertainties,
53 including: (i) environmental effects and landscape processes affecting the sample before
54 extraction; (ii) the methods used in the field to extract the sample; (iii) laboratory techniques
55 applied to extract and quantify data from the core; and (iv) quantitative analyses applied to the
56 data (Table 1). Environmental processes and observation error can affect the representation of
57 species in the data (e.g., their observed relative abundances; Goring et al. 2013). Sub-sampling
58 strategies may alter the chronological placement of events (Liu et al. 2012; Parnell et al. 2008).
59 Manipulation of data, such as interpolation to satisfy statistical assumptions, can introduce
60 statistical artifacts and increase type-I error rates. Such uncertainties affect the robustness of
61 statistical methods and the inferences we may draw from them.

62



Table 1: Sources of uncertainty from pre-sampling natural processes to statistical analyses of data. Uncertainties are not independent across categories and can propagate through the observational process and subsequent analyses.

Source of Uncertainty	Examples
Physical, chemical and biological processes acting on the core or proxy. Not introduced by the observer.	Hiatuses, catchment erosion, variable sedimentation rates and mixing, bioturbation, changing sources of sediment or peat over time, preservation and taphonomy, occurrence of proxy in sample vs actual abundance, differential preservation of proxies.
Observer introduced error from sampling collection and protocol.	Core compression during extraction, coring location (within basin or broader geographical context), sample depth/length and replication, core overlap, contamination.
Post-collection methods applied a sample and subsamples.	Contiguous/non-contiguous sub-sampling, sub-sampling resolution/density/thickness, sampling error/noise, proxy selection, taxonomic resolution, count method and proxy specific method error, dating frequency, dating precision and accuracy, observational error in proxy count.
Data processing and interpretation.	Age-depth modelling, radiocarbon calibration, detrending, time-averaging, statistical methods selection, and understanding of proxy responses to environmental drivers.

63 1.2 Pseudoproxy experiments and virtual ecology

64 One method that we can use to assess the influence of uncertainty on statistical methods and
65 associated inferences is virtual ecology (VE) (Zurell et al. 2010). In the VE approach, simulated
66 data are used as testbeds for recreating, in simulation, observational processes. The synthetic data
67 act as an ‘error-free’ benchmark against which to assess simulated observational processes and
68 analytical methods. The underlying concept is that the synthetic data mimic the statistical
69 properties of empirical data without being subject to the same issues of, for example, limited



70 grain size or extent (Smerdon 2012). Similarly, the simulated observational process aims to
71 recreate the statistical properties of the observer, such as the chance of observing a species
72 occurring at low abundances. Here, we adopt a virtual ecological (VE) approach to (i) assess
73 uncertainties introduced by environmental processes and observer-introduced error by simulating
74 data analogous to a sediment core-type sample, and (ii) to virtually recreate environmental
75 processes acting on a core, and the observational methods used to extract data from the core
76 sample. We extend this approach to include simulated environmental process errors that occur
77 before the observational process. Empirical data typically lack an ‘error-free’ control and even
78 high-quality empirical data (e.g., highly resolved proxy data from a laminated lake sediment
79 core) incorporate multiple uncontrollable sources of uncertainty. Virtual experimentation allows
80 for the effects of sources of uncertainty to be explored for their individual and interaction effects
81 in a systematic and controlled way (Smerdon 2012).

82 The VE approach is similar to pseudoproxy experiments where modified observational data or
83 simulated proxy data (‘pseudoproxies’) are used in place of empirical observations (Mann and
84 Rutherford 2002) and analysed in the same way as empirical measurements (e.g. Asena, Perry
85 and Wilmshurst, 2024). Pseudoproxy experiments originate from climatology where they are a
86 method of assessing palaeoclimate reconstructions (Mann and Rutherford 2002; Christiansen,
87 Schmith, and Thejll 2009; Bothe, Wagner, and Zorita 2019) and, here, we apply the same
88 concepts to palaeoecological data. We use the term virtual ecology to describe the approach by
89 which synthetic data are generated, sampled from and analysed in ways comparable to empirical
90 data (Zurell et al. 2010). The term ‘pseudoproxy’ is used to refer to the simulated proxy data
91 themselves. While simulated data cannot substitute entirely for reality, they provide an
92 experimental platform (*sensu* Peck, 2004) with which to better understand the processes that
93 influence the formation and analysis of empirical data.

94 Pseudoproxies have been widely used in climatology (Mann and Rutherford 2002; Bothe,
95 Wagner, and Zorita 2019), but virtually assessing sampling methods and statistical approaches
96 on palaeoecologically relevant data is less common (although see Asena, Perry and Wilmshurst,
97 2024; Blaauw, Bennett, and Christen, 2010; and Benito, Gil-Romera, and Birks, 2020). The lack
98 of understanding around uncertainties in palaeoecological data has raised concerns regarding the
99 reliability of inferences drawn from them (Blaauw 2012; Blaauw, Christen, and Aquino-López
100 2020). We address this knowledge gap by:



- 101 (i) generating multivariate pseudoproxy archives (considered analogous to a core
102 sample);
- 103 (ii) introducing environmental uncertainty to the pseudoproxy archives via simulated
104 core mixing;
- 105 (iii) introducing process and observer error by virtually recreating the observational
106 processes of sub-sampling the core and quantifying proxies from the sub-samples;
107 and
- 108 (iv) applying two multivariate statistical methods independently, Fisher's Information
109 (FI) and principal curves (PrC), to analyse the 'error-free' and degraded/sub-
110 sampled data.
- 111 (v) Feature analysis methods (a dimensional reduction method that collapses time-
112 series to a set of metrics) are then applied to each the FI and PrCs separately to
113 quantify the effect of increasing levels of uncertainty on the two example
114 methods.

115 Our overarching aim is to quantify the information loss in palaeoecological analyses from
116 environmental uncertainties and process and observer error and how this influences statistical
117 analysis and inference using such data. We use PrCs and FI as examples that capture the
118 underlying drivers of a system in different ways. PrC's, as a method of indirect gradient analysis,
119 primarily captures the long-term ecosystem trends in the pseudoproxies resulting from the
120 primary driver in the scenarios. FI captures shorter-term variance driven by stochastic processes
121 such as the random walk driver. A better understanding of how individual and combined sources
122 of uncertainty affect statistical results and interpretation can help inform study design (e.g.,
123 determining the number of replicate cores or the sub-sampling resolution needed to detect a
124 signal of interest) and the confidence in the statistical results of a study.

125



126 **2 Methods**

127 **2.1 Simulating pseudoproxies**

128 Pseudoproxies are simulated using the model described in Asena, Perry, and Wilmshurst (2024),
129 following the proxy system model framework (Evans et al. 2013) where a sensor (e.g., terrestrial
130 vegetation) responds to environmental drivers and records that response in an archive such as a
131 lake sediment (in this case a pseudoproxy record). The model consists of four components: (i)
132 environmental driver change over time; (ii) species' niches with respect to the driving
133 environment (the sensor response); (iii) pseudoproxy abundances recording the response to
134 driver change in an archive; and (iv) a representation of the formation of the core. In summary,
135 the model generates archives of pseudoproxies consisting of 200 potential species representing a
136 palaeoecological record free from the process and observer error associated with empirical data.
137 Pseudoproxy abundances are simulated as a response to extrinsic and dynamic environmental
138 drivers with intrinsic variability from disturbance events, introduction to the population via
139 dispersal, and variation in carrying capacity over time. Each species has a tolerance for each
140 environmental driver that, together, defines the species niche and determines the population
141 growth rate of a species at any given time-step as a function of the environmental drivers. If any
142 of the environmental drivers fall outside of a species tolerance to that driver, the species will
143 have a negative growth rate and may eventually become locally extinct. Species that are tolerant
144 of the current environmental conditions can be introduced via dispersal, thus creating a species
145 turnover as conditions change. Simulating 200 species covers a wide range of the driver
146 parameter-space and allows different species assemblages to emerge as driver conditions change.
147 Only a subset of the 200 species exists within their niche (i.e., favourable driver conditions) at
148 any one point in time.

149 Thirty-one replicate models were run for a duration of 5000 time-steps with a burn-in period of
150 500 time-steps applied to allow species to stabilise with respect to the driving environment. The
151 scenario we analyse has two environmental drivers: (i) an abrupt environmental driver switching
152 between constant conditions; and (ii) a random walk driver weighted to 0.15 of the total
153 environmental effect. The magnitude of change in the abrupt driver is insufficient to cause a
154 complete species turnover and generalist species survive the shift in extrinsic conditions. The
155 random walk driver may amplify or dampen the effects of the abrupt driver, but in general is
156 favourable to most species in the system. The parameters for each species are randomised for



157 each replicate model run around the same baseline parameters (supplementary table 2). The
158 results of an additional three scenarios with different environmental drivers can be found in the
159 supplementary information.

160

161 Each simulated core is characterised by simulated age, considered to be one year per time-step,
162 and an increase in depth per time-step. The accumulation rate is represented by a combination of
163 a linear decrease with time, with a smoothed random walk superimposed to represent core
164 compression in addition to landscape variability. Variable sedimentation rates result in a
165 different core length (and accumulation per time-step) for each replicate simulation and change
166 the number of model time-steps included in a sub-sample of one-centimetre thickness. Variable
167 change in depth per time-step is calculated as a smoothed and scaled random walk (similar to
168 Benito, Gil-Romera, and Birks, 2020) representing landscape changes and possible hiatuses. A
169 gradual decrease in depth with age can occur from compaction or compression during extraction
170 (Taranu et al. 2018). The simulated data represent a core-type sample from which sub-samples
171 are taken, proxies quantified, and data analysed similar to real-world core samples. The
172 simulated core is used as an ‘error-free’ benchmark against which methodological and statistical
173 processes are assessed and represent the complete (and un-degraded) absolute abundance of
174 proxy data.

175 **2.2 Degradation and sampling of pseudoproxies**

176 Asena, Perry, and Wilmshurst (2024) describe the three sub-models that generate the
177 pseudoproxy data: (i) a driver model representing the environment in which the archive forms;
178 (ii) a sensor model representing the response of a sensor (e.g., terrestrial vegetation) to the
179 environment; and (iii) an archive model that represents how the response of the sensor is
180 recorded (e.g., as fossil pollen) in a medium such as a sediment core. In this section, we describe
181 three more sub-models: (i) a degradation model representing post-depositional processes
182 affecting the pseudoproxy data (in this case core mixing); (ii) an observational model
183 representing how proxies are quantified from a core sample (here, sub-sampling and the count
184 method applied to slides); and (iii) a statistical model analysing both the ‘error-free’ data and
185 degraded/sampled data. The difference between the analysis of the ‘error-free’ data and
186 degraded/sampled data is then quantified. The pseudoproxy archive from each of the 31 model



187 replicates has three treatments: mixing, sub-sampling and proxy counting, applied at 10 levels
188 each individually and combined. Each of the 31 replicate archives results in 1210 datasets from
189 the ‘error-free’ reference core to the most uncertain.

190 *2.2.1 Virtual mixing: degradation model*

191 Core mixing is applied as a centrally weighted rolling-average over time-windows of the archive
192 ranging from unmixed (the ‘error-free’ benchmark) to a window of 10 time-steps. Simulated
193 mixing is represented as consistent over time, rather than being a depth-dependent process such
194 as bioturbation.

195 *2.2.2 Virtual sub-sampling: observation model*

196 An absolute proxy abundance per time-step is generated by the model and is sub-sampled at
197 regular depth intervals ranging from one to ten centimetres. Each sub-sample has a thickness of
198 one centimetre; the number of time-steps within the sampled thickness is determined by the
199 simulated accumulation rate. If the one-centimetre sub-sample covers multiple time-steps, the
200 proxy abundances in that sub-sample are summed. All sub-sample treatment data are converted
201 to relative abundances before analysis so that the analyses are not influenced by excessive values
202 from the summed proxies of multiple time-steps. When applied in combination with simulated
203 proxy counting, values are converted to relative abundance after the proxy count treatment.

204 *2.2.3 Virtual proxy count: observation model*

205 The process of counting proxies in a sub-sample, e.g., counting a few hundred pollen grains or
206 diatoms on a microscope slide, is simulated by random sampling from the absolute proxy
207 abundances with resolutions increasing from 100 to 1000 by 100. The probability of a proxy
208 occurring in the random sample is based on the abundance of that proxy. The sample is then
209 converted to relative abundances comparable to empirical proxy data. The simulated count
210 treatment is applied to the raw, mixed, and sub-sampled data. Note that increasing levels of
211 uncertainty in the proxy counting treatment are represented by a decrease in the proxy count
212 resolution.

213 **2.3 Quantitative analyses**

214 Fisher’s information (FI) and principal curves (PrCs) are used to analyse each treatment level
215 from each replicate core. Fisher’s information and ordination methods have been suggested as



216 appropriate analyses where there are an unlimited number of input variables of any data type that
217 do not require *a priori* knowledge of the driving state variables of a system (Roberts et al. 2018).
218 To quantify the difference in the FI and PrC among treatment levels feature analysis for time-
219 series (FATs) is used (Nun et al. 2015).

220 Because each replicate core results in 1210 FI time-series and principal curves, FATs is used to
221 extract features from the FI time-series and the distance along the PrCs and condense the
222 information to a few features that are comparable among treatment levels. The Euclidean
223 distance between the extracted and scaled features is used as a measure of distance between
224 treatment levels. The data analysis process is as follows: (i) calculate FI and PrC for each
225 treatment level; (ii) extract features from the FI and PrC outputs; and (iii) calculate the distance
226 between the features of each treatment level (Figure 1).

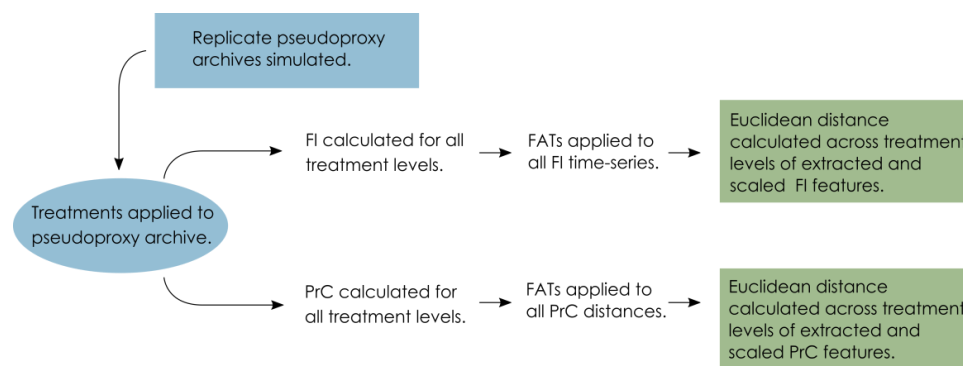


Figure 1: Conceptual data-flow of the degradation, sampling and analysis process.

Treatments of mixing, sub-sampling and proxy counting are applied individually and in combination to the replicate pseudoproxy archives. Fisher's information (FI) and principal curves (PrC) are applied separately to each treatment and subsequently analysed using feature analysis for time-series (FATs). Extracted features are scaled and Euclidean distance between each treatment level and the 'error-free' reference core is calculated.

227 2.3.1 Fisher Information

228 Fisher's information was developed as a method of quantifying information about an unknown
229 parameter from measurable variables (Fisher 1922) and has since been used as a measure of
230 stability in ecosystems (Cabezas and Fath 2002; Mayer, Pawlowski, and Cabezas 2006;



231 Karunanithi et al. 2008; Eason et al. 2016). Fisher's information has been applied to
232 palaeoecological data, with the suggestion that it can be used as an indicator of an approaching
233 regime shift (Spanbauer et al. 2014). Fundamentally, FI evaluates the probability of detecting
234 different system states over time, or the 'stability' of the system; thus, FI changes with the
235 variance in the system. Pseudoproxies from each replicate core, and each level of uncertainty, are
236 analysed using FI, using a custom R package (Asena, Young, and Pletzer 2023).

237 **2.4 Principal curves**

238 Principal curves can be used to identify the underlying variables (e.g., an ecological gradient)
239 that describe a system characterised by multiple state variables and can be considered as a form
240 of non-linear principal components analysis (De'ath 1999). In short, a PrC is a one-dimensional
241 curve fit through the 'middle' of an n -dimensional space (e.g., species composition data; Hastie
242 and Stuetzle, 1989) that can represent species composition by mapping the sites onto a low-
243 dimensional space using similarity or dissimilarity measures. The arrangement of sites reflects
244 the composition of species in the reduced dimension space as the distance between sites is
245 proportional to the distance in species composition (De'ath 1999). Principal curves can be used
246 as a method of gradient analysis, the underlying concept being that the species abundances
247 change in a predictable way along an ecological gradient. Here, we use PrCs to represent change
248 in species composition over time and as a method of indirect gradient analysis using the
249 distances along the PrC. Cubic smoothing splines are used to fit the PrC to the data. Details for
250 the implementation of PrCs can be found in Hastie and Stuetzle (1989), De'ath (1999), and
251 Simpson and Birks (2012). PrC analyses were conducted for all replicate pseudoproxy datasets
252 for each level of increasing uncertainty using the analogue package (Simpson and Oksanen
253 2020) in R (R Core Team 2020).

254 *2.4.1 Feature analysis for time-series*

255 The individual and combined degradation and sampling treatments result in 1210 time-series per
256 replicate, yielding $31 \times 1210 = 37510$ virtual cores per scenario. Thus, to compare the analyses
257 (FI and PrCs) of each pseudoproxy record, as uncertainties are introduced, with the 'error-free'
258 benchmark, we use feature analysis to reduce the dimensions of the time-series for comparison
259 across treatment levels.



260 Features are extracted from the FI time-series and the distances along the PrCs drawing on
261 feature analysis for time-series (FATs) (Richards et al. 2011; Kim et al. 2011; Nun et al. 2015;
262 Sokolovsky et al. 2017) and change point analysis (Killick and Eckley 2014) to describe the FI
263 and PrC analyses as a series of metrics. Sixty-two features are extracted from the FI time-series
264 and PrC (supplementary table 4). Describing the FI time-series and PrC as a series of
265 metrics/features allows comparison between treatments by calculating a distance measure (we
266 use Euclidean distance) between the extracted features of each treatment level. The feature
267 analysis process is as follows:

- 268 1. Features are extracted from the FI time-series and distances along the PrCs for all
269 replicate model runs of the ‘error-free’ archive.
- 270 2. A correlation matrix of the features from the replicate ‘error-free’ datasets is constructed,
271 and features with an absolute Pearson’s correlation coefficient greater than $|0.7|$ are
272 excluded sequentially, recalculating the correlation matrix until all highly correlated
273 features are dropped, starting with the highest correlation coefficient (Dormann et al.
274 2007).
- 275 3. The remaining features (with an absolute Pearson’s correlation coefficient less than $|0.7|$)
276 are then calculated for all replicates across all treatment levels, resulting in a number
277 (ranging between 14-26 per scenario) of single metric features per treatment that describe
278 the FI time-series and PrC.
- 279 4. The features are scaled (by subtracting the mean of the entire series from each point and
280 dividing it by the series’ standard deviation), and the Euclidean distance is calculated
281 across treatment levels, resulting in a single distance measure between the ‘error-free’
282 core and each treatment level.
- 283 5. Summaries of the Euclidean distances are calculated for all treatment levels across
284 replicates resulting in a single distance measure for each treatment from the ‘error-free’
285 benchmark.

286



287 **3 Results**

288 **3.1 Effects of individual sources of uncertainty**

289 In the extracted features for FI, sub-sampling causes the largest overall increase in the median
290 Euclidean distance from the ‘error-free’ core, followed by proxy counting and then mixing;
291 however, there is some overlap in the confidence envelopes across all three treatments (Figure 2
292 A). Distance increases consistently with uncertainty in the mixing treatment, showing a steeper
293 increase in distance across uncertainty compared with the other two treatments. Between
294 successive treatment levels, proxy counting shows little increase in the median Euclidean
295 distance as uncertainty increases. In the sub-sampling treatment, distance increases more in the
296 lower uncertainty levels than higher levels, potentially plateauing at higher uncertainty (Figure 2
297 A). A degree of variability is visible across the treatment levels resulting from the stochasticity in
298 the underlying model and simulated observational processes (i.e., proxy counting is a random
299 sampling process, and sub-sampling is dependent on the variable accumulation rates of the core).

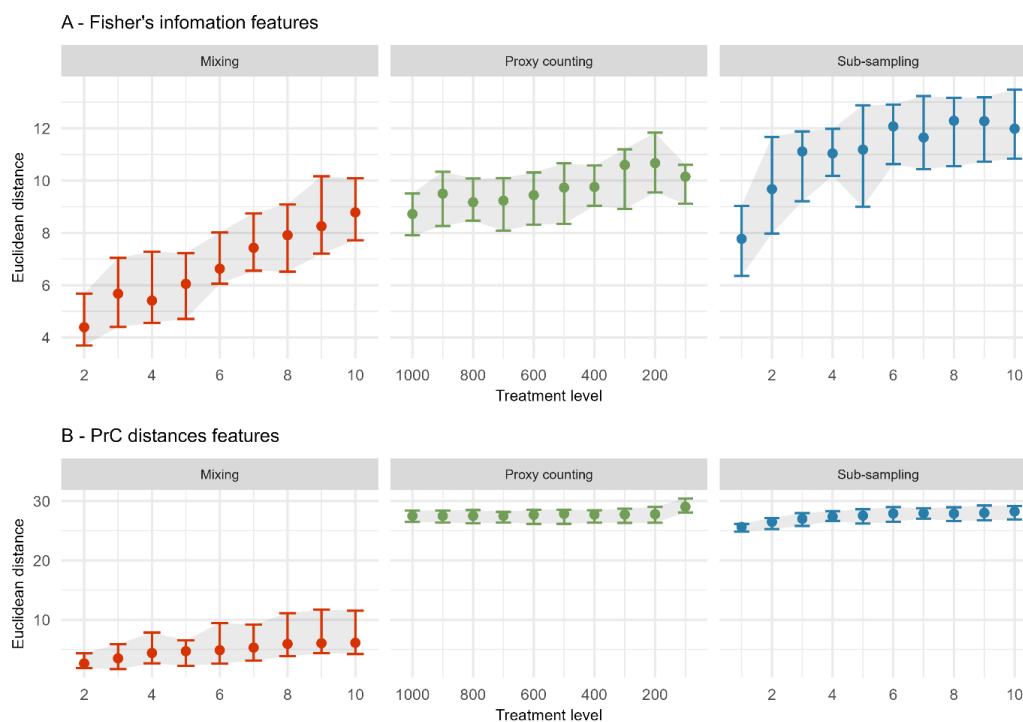


Figure 2: The median (dots), 25th, and 75th quantiles (error-bars and shaded area) of the Euclidean distance from the 'error-free' core of features extracted from the Fisher's information (A) and PrC distances (B) calculated across replicate simulations. Note the x-axis is organised so uncertainty consistently increases from left-to-right.

300 In the analysis of the PrC features, across all scenarios the least effect on median Euclidean
 301 distance is observed in the mixing treatment (Figure 2 B). Proxy counting and sub-sampling
 302 have overlapping confidence envelopes, although they are much smaller than those of the mixing
 303 treatment. Proxy counting shows no consistent pattern in median Euclidean distance between
 304 successive treatment levels until the lowest count resolution. Conversely, the sub-sampling
 305 treatment shows an increase in the lower treatment levels, plateauing as sub-sampling interval
 306 increases (Figure 2 B).

307



308 **3.2 Effects of two combined sources of uncertainty**

309 Looking at individual treatment effects, the distance of the extracted features increases with the
310 severity of the treatment levels. In the following section, treatments are applied simultaneously
311 to determine which combinations cause the greatest effect on analyses of the core. The greatest
312 increase in mean Euclidean distance on the features extracted from FI from the ‘error-free’ core
313 arises from the interaction of the sub-sampling and proxy counting uncertainties increasing
314 together (i.e., along the diagonal; Figure 3 A) with a stronger effect from the subsampling
315 treatment. Mixing combined with sub-sampling or with proxy counting, shows no clear
316 interaction effect as the treatments increase in severity together. The smallest increase in distance
317 is from the combination of mixing with proxy counting, suggesting that sub-sampling tends to
318 have the greatest influence of the three treatments (Figure 3 A). The effect of the mixing
319 treatment on the mean Euclidean distance is small when compared to those of either sub-
320 sampling or proxy counting (Figure 3 A). Variability across the surface of each plot emerge from
321 underlying model stochasticity, random sampling in the simulated count method, and the
322 variable accumulation rates of the replicate cores.

323

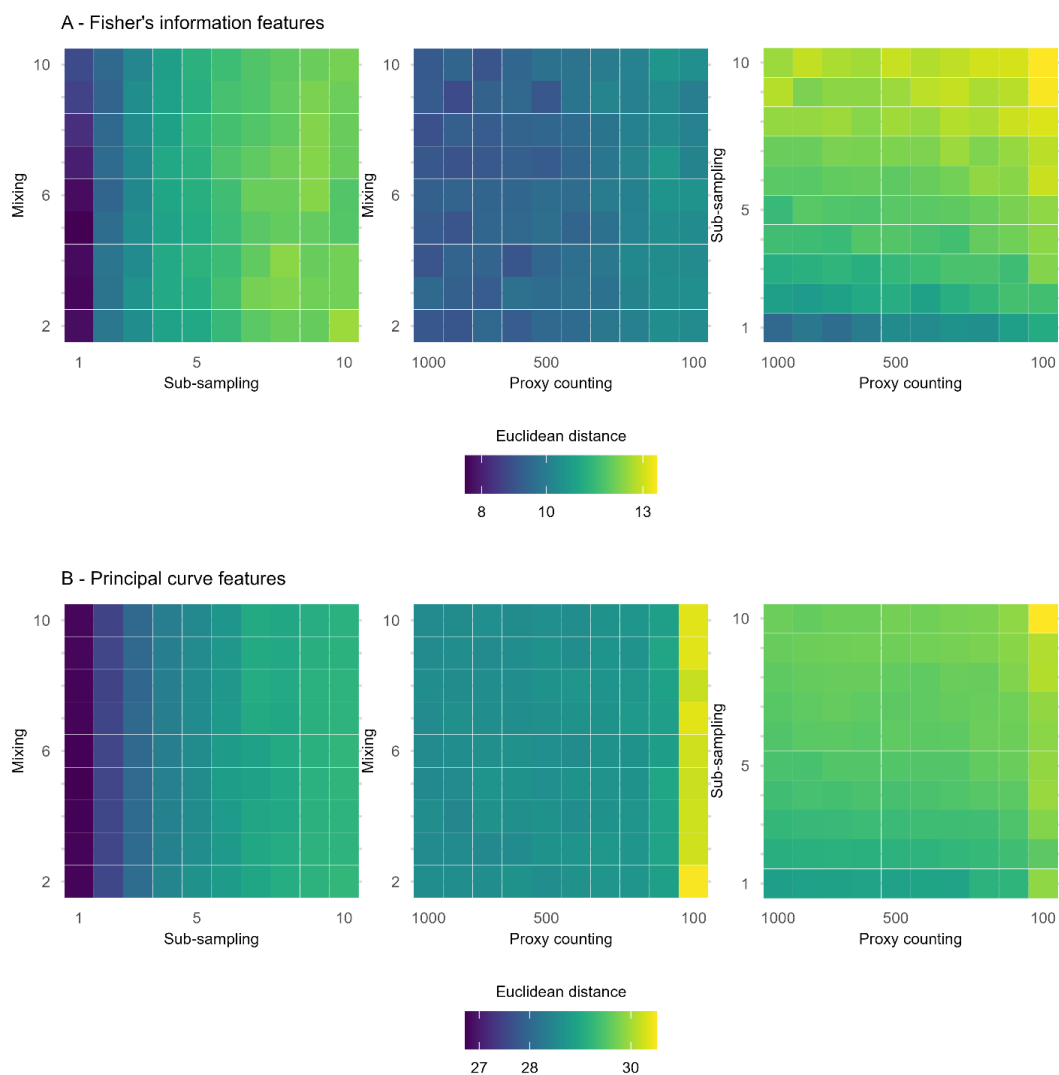


Figure 3: Mean Euclidean distance of features from the ‘error-free’ core of two treatments combined calculated across replicate simulations for Fisher’s information (A) and principal curves (B). The mixing axis shows the number of time-steps over which mixing occurs. Along the sub-sampling axis, the frequency of sub-sampling in centimetres is shown, and the proxy counting axis displays count resolutions in number of individuals counted per sample. In the proxy counting treatment, uncertainty increases as count resolution decreases.



324 In the extracted features from the distances along the PrCs, the combined effects of sub-sampling
325 with proxy counting show the largest increase in the mean Euclidean distance of all the
326 combined treatments, with a weak interaction effect as proxy count and sub-sampling
327 uncertainties increase together (Figure 3 B). No interaction effect is visible in either the
328 combined treatments of mixing with sub-sampling or mixing with proxy counting (Figure 3 B).

329 **3.3 Effects of three combined sources of uncertainty**

330 The interaction effects of all three uncertainties applied simultaneously are assessed for the
331 extracted FI and PrC features (Figure 4). An interaction effect is visible in the increase of mean
332 Euclidean distance as the sub-sampling interval increases (along the x -axis), together with proxy
333 counting resolution decreasing (across facets from top left to bottom right); however, no clear
334 increase is visible along the mixing axis, indicating little contribution from mixing to the
335 interaction of the three treatments (Figure 4). Overall, the greatest increase in the mean
336 Euclidean distance among treatments is at the lowest proxy count and largest sub-sampling
337 interval.

338

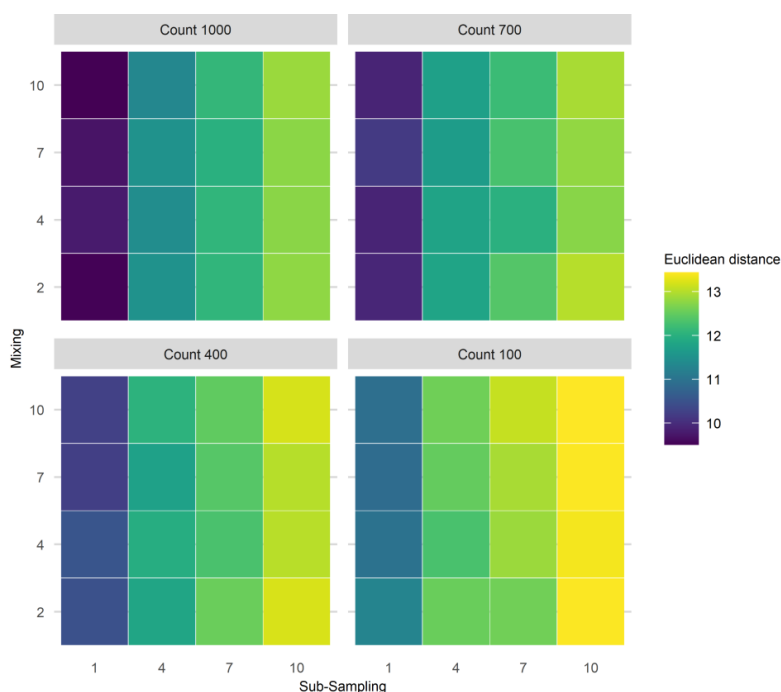


Figure 4: Mean Euclidean distance from the ‘error-free’ core for three treatments applied in combination. To demonstrate the three treatment dimensions, results are displayed such that each plot axis shows mixing (number of time-steps over which mixing occurs) and sub-sampling (frequency in centimetres) treatments, and each facet (sub-plot) is the proxy counting treatment (number of individuals counted in sub-sample). Uncertainty from proxy counting increases from the top left to the bottom right.

339 In the PrC features, applying three treatments in combination does not show a clear three-way
 340 interaction as uncertainty increases (Figure 3.4). An increase in mean Euclidean distance is
 341 visible along the sub-sampling axis (as sub-sampling interval increases), but there is little visible
 342 effect of the proxy counting treatment (reducing in resolution across facets from top left to
 343 bottom right) until the lowest resolution. Mixing contributes relatively little to the overall
 344 increase in mean Euclidean distance showing no visible increase along the mixing axis (Figure
 345 3.4).

346

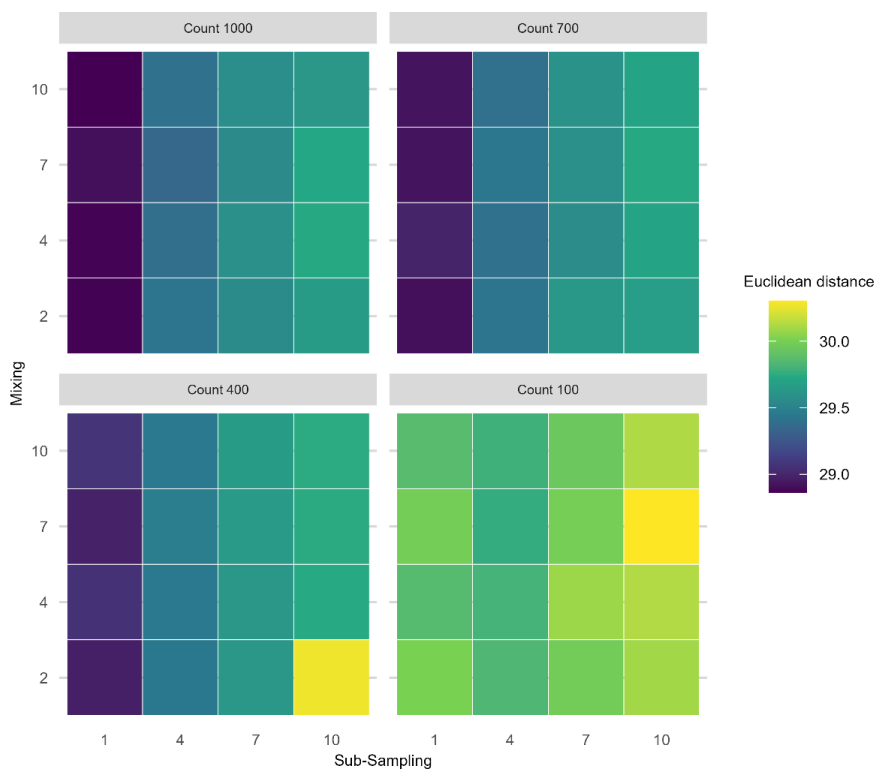


Figure 5: Mean Euclidean distance from the ‘error-free’ core of all uncertainties increasing in combination. Proxy count resolution decreases across facets from top left to bottom right. Within each facet the axes show the sub-sampling (frequency in centimetres) and mixing treatments (number of time-steps).

347



348 **4 Discussion**

349 Our goal in this paper is to address how process and observer error affect statistical methods
350 applied to palaeoecological data and the inferences we draw from them. Here, we have assessed
351 some of the uncertainties that affect species proxy data. Additionally, uncertainty arises from
352 building chronologies (Blaauw et al., 2018; Parnell et al., 2008; Telford et al., 2004) and
353 measuring abiotic system variables, such as isotopic records and lake level reconstructions,
354 which carry their own uncertainties. To draw reliable conclusions from palaeoecological data, it
355 is crucial to view our inferences in the context of the uncertainties they integrate.

356 **4.1 Effects of individual sources of uncertainty**

357 Without exception, sub-sampling treatments show the largest effect on the median Euclidean
358 distances of the FI features (although, with some overlap in the confidence envelope with the
359 proxy counting treatment), followed by the proxy counting process. For the PrC features, both
360 sub-sampling and proxy counting treatments show a similar magnitude of effect on Euclidean
361 distance. For both the FI and PrC features, the smallest effect on Euclidean distance between the
362 ‘error-free’ and degraded cores is from the simulated mixing degradation process.

363 Perhaps the most interesting implication of our analyses in the context of empirical ecology is
364 how the effects of sources of error differ between the two statistical metrics (FI and PrC).
365 Beyond the initial increase in Euclidean distance in the PrC from the application of proxy
366 counting and sub-sampling (an unavoidable cost), there was little further effect until the lowest
367 proxy count and sub-sampling resolutions. Thus, PrCs may be a useful measure of a system’s
368 trajectory for patchy data (e.g., initial analysis of low sub-sampling resolution data before
369 deciding where to focus sampling effort). For FI, treatment effects have a more consistent
370 increase in distance from the ‘error-free’ core with treatment intensity. The short-term variability
371 captured by FI may provide useful system indicators (*sensu* Eason and Cabezas, 2012) but may
372 also require high-quality data (e.g., high sub-sampling resolution and proxy counting) for reliable
373 inferences. The required temporal resolution of the data is also likely to increase if accumulation
374 rates are slow and species turnover is rapid. Increased sub-sampling frequency is required in
375 systems that change rapidly compared with more stable systems where the difference between
376 successive time-steps is small. Slow accumulation rates mean that a one-centimetre-thick sub-
377 sample integrates multiple years of ecological change; thus, uncertainty from sub-sampling



378 resolution will increase if the accumulation rate is slow and ecological change is rapid. An
379 observer may interpret FI results with the knowledge of which sources of uncertainty, whether
380 controllable (e.g., sub-sampling and proxy counting resolution) or uncontrollable (e.g., mixing
381 and accumulation rates), have the greatest influence. After introducing uncertainties the primary
382 patterns, such as long periods of increase in FI, remain visible and offer a useful depiction of
383 community change.

384 **4.2 Effects of combined sources of uncertainty**

385 For both FI and PrC, when two treatments are applied in combination, the greatest overall
386 increase in mean Euclidean distance from the ‘error-free’ core resulted from sub-sampling
387 uncertainty in combination with proxy counting uncertainty. Although for the PrC the maximum
388 increase in mean Euclidean distance for two simultaneous treatments occurred at the lowest
389 proxy count resolution in combination with mixing, such a low proxy count resolution is unlikely
390 in any empirical study. In our analyses, mixing has relatively little effect compared with sub-
391 sampling or proxy counting and the effect tends to be obscured by other sources of stochasticity
392 (disturbance, dispersal, and temporal changes in carrying capacity), variable accumulation rates,
393 and randomised sampling of the proxy abundances.

394 In the case of FI, the greatest benefit in terms of reducing the distance from the ‘error-free’ core,
395 is derived from increasing sub-sampling resolution followed by proxy count resolution.
396 However, from the standpoint of an observer, increasing the resolution of an FI time-series may
397 not increase the information content, at least in terms of capturing long-term patterns. Simple
398 driving environments (e.g., the single driver simulations) are likely to be adequately represented
399 by FI applied to low-resolution data, and interpretation of FI from complex driving environments
400 (i.e., those influenced by multiple drivers) is potentially challenging without considerable
401 knowledge of the underlying driving conditions. The benefit of the VE approach is that it allows
402 us to examine how the underlying dynamics manifest in multivariate indicators of change such as
403 FI; however, such near-complete information is rarely, if ever, available. Ultimately, an observer
404 must base decisions, such as sub-sampling strategy, on their specific aims. If accurate evaluation
405 of short-term variability is a requirement (e.g., for studies of ecosystem resilience), then
406 dedicating resources to sub-sampling resolution is likely to be beneficial to analyses such as FI.
407 Reducing observer error, a more controllable source of error, may help detect a short-term signal



408 of interest if the uncontrollable sources of error, such as sediment accumulation rates, mixing,
409 and driver variability, are sufficiently small that the signal remains detectable.

410 PrC shows little increase in distance (after the initial increase from the application of the
411 treatments) from the ‘error-free’ reference with combined treatment levels. Thus, as a
412 representation of compositional change, it may be robust to low-resolution data (e.g., infrequent
413 sub-sampling). Short-term changes in abundance (e.g., small disturbances) will likely become
414 less evident in the PrC; however, our results suggest that overall patterns seen in a PrC are robust
415 to multiple sources of error. Thus, from the perspective of an observer, high-resolution data may
416 only be required for PrC to identify short-term compositional changes, such as perturbations that
417 take a few generations to recover from.

418 **4.3 Implications for empirical studies**

419 One purpose of using virtual ecology to estimate the influence of sources of uncertainty on
420 quantitative analyses is to understand what can be done to mitigate their effects and where to
421 focus limited resources, such as time spent analysing an individual core. Trade-offs are inherent
422 in any sampling design. For example, is it more advantageous to focus effort on spatial coverage
423 by taking multiple cores rather than increasing sub-sampling resolution on fewer cores? Such
424 questions, of course, depend on the intention of the study and knowledge of the study site/system
425 (i.e., some knowledge of the uncertainties that will be encountered such as landscape changes
426 through time). Virtual ecology allows us to make a more informed decision about what field and
427 laboratory methods, and quantitative analyses will be most appropriate given the question of
428 interest. For example, if analysing a network of core data over a large geographic region, where
429 the observer is interested in the spatial consistency of the system’s trajectory but does not have
430 the resources to extract highly resolved data from each core, methods such as PrC may be more
431 informative than FI. Conversely, if an observer is interested in short-term change in a single core
432 (or a region of particular interest in a core) it may be worth allocating the time to extracting
433 highly resolved data to increase the reliability of analyses sensitive to variance such as FI. Of
434 course, FI and PrC are only two examples of a suite of available statistical analyses (Birks et al.
435 2012; Blaauw, Christen, and Aquino-López 2020) and an observer should apply more than one.
436 However, PrC and FI provide different representations of a system’s trajectory. Principal curves
437 reflect the system’s overall trajectory (De’ath 1999) and, as a form of indirect gradient analysis,
438 PrC reflects the primary driver of the scenario. In contrast, FI is more sensitive to short-term



439 variability (Eason et al. 2016) and so reflects driver interactions. Although FI does capture the
440 long-term system trajectory, these trends can be obscured by short-term variability such as that
441 caused by the random walk driver. Similar analyses (e.g., other ordination methods) may be
442 affected by sources of uncertainty in similar ways.

443 Alongside considerations of the sensitivity of analyses to uncertainty, are questions of how
444 sensitive different proxies are to driver change and, consequently, how informative the analyses
445 are. The question of how different proxies respond to drivers at different temporal and spatial
446 scales remains largely unanswered. Interestingly, the sensitivity of different proxies to
447 environmental change may be ecosystem specific. Phytoliths have been reported as more
448 sensitive than pollen to changes in dry forests with the reverse being true of evergreen forests at
449 a site in Bolivia (Plumpton, Whitney, and Mayle 2019). In savannahs pollen and phytoliths have
450 been shown to be equally sensitive to changes in the environment (Plumpton, Whitney, and
451 Mayle 2019). Thus, ecosystem-specific and proxy-specific knowledge are important
452 considerations, as increasing sub-sampling efforts to obtain a higher resolution representation of
453 change from numerical analyses may not be useful if the proxy is not a reliable sensor at that
454 resolution. Furthermore, compositional change is not the sole (or necessarily the most
455 appropriate) measure of system change, and other measures such as body size distributions,
456 physiognomic, and functional and phylogenetic diversity can be included (Goring et al. 2013;
457 Reitalu et al. 2015; Clements and Ozgul 2016; Spanbauer et al. 2016; Adeleye et al. 2023).

458 **5 Conclusion**

459 Palaeoecological uncertainty can be considered at four levels: environmental processes, field
460 methods, laboratory methods, and quantitative analyses (Table 1). The effects of different
461 sources of uncertainty are challenging to disentangle and quantify from empirical studies alone,
462 and virtual ecology provides a useful approach as different uncertainties can be manipulated.
463 However, virtual ecology has its own set of limitations. The data degradation and sampling
464 processes described here still represent a relatively ideal situation in that the timespan of the data
465 is long relative to the driving processes, and the sub-sampling treatment is at regular depth
466 intervals. The representation of mixing is also simple in that it is applied consistently down the
467 core. Thus, investigation of uncertainty through both empirical and virtual approaches is
468 necessary to better understand the influence of process and observer error on the analysis of
469 palaeoecological data. Empirical approaches could involve collecting high-quality data (e.g.,



470 well-dated sediment cores with frequent sub-sampling resolution), ideally with replicate cores
471 from the same location, to use as a benchmark against which to assess analyses when sub-
472 sampling resolution is reduced (e.g., Liu et al., 2012). Experimental approaches might include
473 laboratory and *in situ* manipulation; for example, Payne and Gehrels (2010) monitor the
474 movement of tephra in the field and under controlled laboratory environments to understand the
475 influence of tephra taphonomy on tephrochronology. Finally, combined empirical-virtual
476 approaches could be developed using (virtually) modified empirical data; for example, applying
477 a simulated mixing process to empirical sediment core data (such as those from varved sediments
478 that are subject to minimal mixing) and assessing the subsequent analyses. Mann and Rutherford
479 (2002) demonstrate this approach by generating pseudoproxy data by subjecting instrumental
480 data to degradation, such as various noise processes and spatial sampling strategies, to assess sea
481 surface temperature reconstruction methods. They used simulation to create a continuous sea
482 surface temperature record from the patchier instrumental data before applying the degradation
483 processes. Although the implications of such methods are different for ecological data, similar
484 approaches could fruitfully be applied. A better understanding of the proxy system models of
485 different proxies (i.e., how different proxies record environmental signals in an archive) and the
486 uncertainties around quantifying and analysing proxy data can bring us closer to understanding
487 long-term climate and ecosystem dynamics.

488

489

490

491 **Acknowledgements**

492 The authors are very grateful for the support of the Centre for eResearch, particularly Nick
493 Young and Noel Zeng for their digital research expertise. We also acknowledge the New
494 Zealand eScience Infrastructure (NeSI) for the use of their computational resources, without
495 which the scale of the analyses involved in this paper would not have been possible. Callum
496 Walley and Anthony Shaw of NeSI provided instrumental support for high-performance
497 computing. Finally, we extend our thanks to members of the Perry Lab for helping shape the
498 project.



499 **Data availability**

500 Functions used for Feature Analysis for Time-series, and other calculated metrics can be found
501 here: <https://doi.org/10.5281/zenodo.8052806>.

502

503 **Author contributions**

504 Quinn Asena contributed to the conceptualization, methodology, and writing the original draft.
505 George Perry contributed to the conceptualization, methodology, and reviewing and editing the
506 manuscript, providing supervision and statistical expertise. Janet Wilmshurst provided
507 palaeoecological expertise to the project, and reviewed and edited the manuscript.

508 **Competing interests**

509 The authors declare that they have no conflict of interest.

510 **Funding**

511 The author(s) disclosed receipt of the following financial support for the research, authorship,
512 and/or publication of this article: This work was conducted through the New Zealand's
513 Biological Heritage National Science Challenge, which is funded by the New Zealand Ministry
514 of Business, Innovation and Employment.

515

516 **References**

517 Adesanya Adeleye, M., Charles Andrew, S., Gallagher, R., van der Kaars, S., De Deckker, P.,
518 Hua, Q., Haberle, S.G., 2023. On the timing of megafaunal extinction and associated floristic
519 consequences in Australia through the lens of functional palaeoecology. *Quaternary Science*
520 *Reviews* 316, 108263. <https://doi.org/10.1016/j.quascirev.2023.108263>

521 Asena, Quinn, George LW Perry, and Janet M Wilmshurst. 2024. "Is the Past Recoverable from
522 the Data? Pseudoproxy Modelling of Uncertainties in Palaeoecological Data." *The Holocene*,
523 May, 09596836241247304. <https://doi.org/10.1177/09596836241247304>.



- 524 Asena, Quinn, Nick Young, and Alex Pletzer. 2023. “UoA-eResearch/fisheR: V1.0.0.” Zenodo.
525 <https://doi.org/10.5281/ZENODO.8052806>.
- 526 Beck, Kristen K., Michael-Shawn Fletcher, Patricia S. Gadd, Henk Heijnis, Krystyna M.
527 Saunders, Gavin L. Simpson, and Atun Zawadzki. 2018. “Variance and Rate-of-Change as Early
528 Warning Signals for a Critical Transition in an Aquatic Ecosystem State: A Test Case from
529 Tasmania, Australia.” *Journal of Geophysical Research: Biogeosciences* 123 (2): 495–508.
530 <https://doi.org/10.1002/2017JG004135>.
- 531 Benito, Blas M., Graciela Gil-Romera, and H. John B. Birks. 2020. “Ecological Memory at
532 Millennial Time-Scales: The Importance of Data Constraints, Species Longevity and Niche
533 Features.” *Ecography* 43 (1): 1–10. <https://doi.org/10.1111/ecog.04772>.
- 534 Birks, John B. H., André F. Lotter, Steve Juggins, and John P. Smol. 2012. *Tracking
535 Environmental Change Using Lake Sediments: Data Handling and Numerical Techniques*.
536 Springer Science & Business Media.
- 537 Blaauw, Maarten. 2012. “Out of Tune: The Dangers of Aligning Proxy Archives.” *Quaternary
538 Science Reviews, The INTEgration of Ice Core, Marine and TERrestrial Records of the Last
539 Termination (INTIMATE) 60,000 to 8000 BP*, 36 (March): 38–49.
540 <https://doi.org/10.1016/j.quascirev.2010.11.012>.
- 541 Blaauw, Maarten, K. D. Bennett, and J. Andrés Christen. 2010. “Random Walk Simulations of
542 Fossil Proxy Data.” *The Holocene* 20 (4): 645–49. <https://doi.org/10.1177/0959683609355180>.
- 543 Blaauw, Maarten, J. Andrés Christen, and Marco Antonio Aquino-López. 2020. “A Review of
544 Statistics in Palaeoenvironmental Research.” *Journal of Agricultural, Biological and
545 Environmental Statistics* 25 (1): 17–31. <https://doi.org/10.1007/s13253-019-00374-2>.
- 546 Bothe, Oliver, Sebastian Wagner, and Eduardo Zorita. 2019. “Simple Noise Estimates and
547 Pseudoproxies for the Last 21000 Years.” *Earth System Science Data* 11 (3): 1129–52.
548 <https://doi.org/10.5194/essd-11-1129-2019>.
- 549 Cabezas, Heriberto, and Brian D. Fath. 2002. “Towards a Theory of Sustainable Systems.” *Fluid
550 Phase Equilibria*, Proceedings of the Ninth International Conference on Properties and Phase



- 551 Equilibria for Product and Process Design, 194–197 (March): 3–14.
552 [https://doi.org/10.1016/S0378-3812\(01\)00677-X](https://doi.org/10.1016/S0378-3812(01)00677-X).
- 553 Christiansen, Bo, T. Schmith, and P. Thejll. 2009. “A Surrogate Ensemble Study of Climate
554 Reconstruction Methods: Stochasticity and Robustness.” *Journal of Climate* 22 (4): 951–76.
555 <https://doi.org/10.1175/2008JCLI2301.1>.
- 556 Clements, Christopher F., and Arpat Ozgul. 2016. “Including Trait-Based Early Warning Signals
557 Helps Predict Population Collapse.” *Nature Communications* 7 (1).
558 <https://doi.org/10.1038/ncomms10984>.
- 559 De’ath, Glenn. 1999. “Principal Curves: A New Technique for Indirect and Direct Gradient
560 Analysis.” *Ecology* 80 (7): 2237–53. [https://doi.org/10.1890/0012-9658\(1999\)080\[2237:PCANTF\]2.0.CO;2](https://doi.org/10.1890/0012-9658(1999)080[2237:PCANTF]2.0.CO;2).
- 562 Dormann, Carsten F., Jana M. McPherson, Miguel B. Araújo, Roger Bivand, Janine Bolliger,
563 Gudrun Carl, Richard G. Davies, et al. 2007. “Methods to Account for Spatial Autocorrelation in
564 the Analysis of Species Distributional Data: A Review.” *Ecography* 30 (5): 609–28.
565 <https://doi.org/10.1111/j.2007.0906-7590.05171.x>.
- 566 Eason, Tarsha, and Heriberto Cabezas. 2012. “Evaluating the Sustainability of a Regional
567 System Using Fisher Information in the San Luis Basin, Colorado.” *Journal of Environmental
568 Management* 94 (1): 41–49. <https://doi.org/10.1016/j.jenvman.2011.08.003>.
- 569 Eason, Tarsha, Ahjond S. Garmestani, Craig A. Stow, Carmen Rojo, Miguel Alvarez-Cobelas,
570 and Heriberto Cabezas. 2016. “Managing for Resilience: An Information Theory-Based
571 Approach to Assessing Ecosystems.” *Journal of Applied Ecology* 53 (3): 656–65.
572 <https://doi.org/10.1111/1365-2664.12597>.
- 573 Evans, M. N., S. E. Tolwinski-Ward, D. M. Thompson, and K. J. Anchukaitis. 2013.
574 “Applications of Proxy System Modeling in High Resolution Paleoclimatology.” *Quaternary
575 Science Reviews* 76 (September): 16–28. <https://doi.org/10.1016/j.quascirev.2013.05.024>.
- 576 Fisher, R. A. 1922. “On the Mathematical Foundations of Theoretical Statistics.” *Philosophical
577 Transactions of the Royal Society of London. Series A, Containing Papers of a Mathematical or
578 Physical Character* 222: 309–68.



- 579 Goring, Simon, Terri Lacourse, Marlow G. Pellatt, and Rolf W. Mathewes. 2013. “Pollen
580 Assemblage Richness Does Not Reflect Regional Plant Species Richness: A Cautionary Tale.”
581 Edited by Amy Austin. *Journal of Ecology* 101 (5): 1137–45. [https://doi.org/10.1111/1365-
582 2745.12135](https://doi.org/10.1111/1365-2745.12135).
- 583 Hastie, Trevor, and Werner Stuetzle. 1989. “Principal Curves.” *Journal of the American
584 Statistical Association* 84 (406): 502–16. <https://doi.org/10.1080/01621459.1989.10478797>.
- 585 Jackson, Stephen T. 2007. “Looking Forward from the Past: History, Ecology, and
586 Conservation.” *Frontiers in Ecology and the Environment* 5 (9): 455–55.
587 [https://doi.org/10.1890/1540-9295\(2007\)5\[455:LFFTPH\]2.0.CO;2](https://doi.org/10.1890/1540-9295(2007)5[455:LFFTPH]2.0.CO;2).
- 588 Karunanithi, Arunprakash T., Heriberto Cabezas, B. Roy Frieden, and Christopher W.
589 Pawlowski. 2008. “Detection and Assessment of Ecosystem Regime Shifts from Fisher
590 Information.” *Ecology and Society* 13 (1).
- 591 Killick, Rebecca, and Idris A. Eckley. 2014. “Changepoint: An r Package for Changepoint
592 Analysis.” *Journal of Statistical Software* 58 (1): 1–19. <https://doi.org/10.18637/jss.v058.i03>.
- 593 Kim, Dae-Won, Pavlos Protopapas, Yong-Ik Byun, Charles Alcock, Roni Khardon, and Markos
594 Trichas. 2011. “Quasi-Stellar Object Selection Algorithm Using Time Variability and Machine
595 Learning: Selection of 1620 Quasi-Stellar Object Candidates from Macho Large Magellanic
596 Cloud Database.” *The Astrophysical Journal* 735 (2): 68. [https://doi.org/10.1088/0004-
597 637X/735/2/68](https://doi.org/10.1088/0004-637X/735/2/68).
- 598 Kosnik, Matthew A., and Michał Kowalewski. 2016. “Understanding Modern Extinctions in
599 Marine Ecosystems: The Role of Palaeoecological Data.” *Biology Letters* 12 (4).
600 <https://doi.org/10.1098/rsbl.2015.0951>.
- 601 Liu, Yao, Simon Brewer, Robert K. Booth, Thomas A. Minckley, and Stephen T. Jackson. 2012.
602 “Temporal Density of Pollen Sampling Affects Age Determination of the Mid-Holocene
603 Hemlock (Tsuga) Decline.” *Quaternary Science Reviews* 45 (June): 54–59.
604 <https://doi.org/10.1016/j.quascirev.2012.05.001>.



- 605 Mann, Michael E., and Scott Rutherford. 2002. "Climate Reconstruction Using
606 'Pseudoproxies'." *Geophysical Research Letters* 29 (10): 139-1-139-4.
607 <https://doi.org/10.1029/2001GL014554>.
- 608 Mayer, Audrey L., Christopher W. Pawlowski, and Heriberto Cabezas. 2006. "Fisher
609 Information and Dynamic Regime Changes in Ecological Systems." *Ecological Modelling*,
610 Selected Papers from the Third Conference of the International Society for Ecological
611 Informatics (ISEI), August 26–30, 2002, Grottaferrata, Rome, Italy, 195 (1): 72–82.
612 <https://doi.org/10.1016/j.ecolmodel.2005.11.011>.
- 613 Nun, Isadora, Pavlos Protopapas, Brandon Sim, Ming Zhu, Rahul Dave, Nicolas Castro, and
614 Karim Pichara. 2015. "FATS: Feature Analysis for Time Series." *arXiv:1506.00010*, August.
615 <https://arxiv.org/abs/1506.00010>.
- 616 Parnell, A. C., J. Haslett, J. R. M. Allen, C. E. Buck, and B. Huntley. 2008. "A Flexible
617 Approach to Assessing Synchronicity of Past Events Using Bayesian Reconstructions of
618 Sedimentation History." *Quaternary Science Reviews* 27 (19): 1872–85.
619 <https://doi.org/10.1016/j.quascirev.2008.07.009>.
- 620 Payne, Richard, and Maria Gehrels. 2010. "The Formation of Tephra Layers in Peatlands: An
621 Experimental Approach." *CATENA* 81 (1): 12–23. <https://doi.org/10.1016/j.catena.2009.12.001>.
- 622 Peck, Steven L. 2004. "Simulation as Experiment: A Philosophical Reassessment for Biological
623 Modeling." *Trends in Ecology & Evolution* 19 (10): 530–34.
624 <https://doi.org/10.1016/j.tree.2004.07.019>.
- 625 Plumpton, Heather, Bronwen Whitney, and Francis Mayle. 2019. "Ecosystem Turnover in
626 Palaeoecological Records: The Sensitivity of Pollen and Phytolith Proxies to Detecting
627 Vegetation Change in Southwestern Amazonia." *The Holocene* 29 (1): 1720–30.
628 <https://doi.org/10.1177/0959683619862021>.
- 629 R Core Team. 2020. "R: A Language and Environment for Statistical Computing." Vienna,
630 Austria.
- 631 Reitalu, Triin, Pille Gerhold, Anneli Poska, Meelis Pärtel, Vivika Väli, and Siim Veski. 2015.
632 "Novel Insights into Post-Glacial Vegetation Change: Functional and Phylogenetic Diversity in



- 633 Pollen Records.” Edited by Otto Wildi. *Journal of Vegetation Science* 26 (5): 911–22.
634 <https://doi.org/10.1111/jvs.12300>.
- 635 Richards, Joseph W., Dan L. Starr, Nathaniel R. Butler, Joshua S. Bloom, John M. Brewer, Arien
636 Crellin-Quick, Justin Higgins, Rachel Kennedy, and Maxime Rischard. 2011. “On Machine-
637 Learned Classification of Variable Stars with Sparse and Noisy Time-Series Data.” *The*
638 *Astrophysical Journal* 733 (1): 10. <https://doi.org/10.1088/0004-637X/733/1/10>.
- 639 Roberts, Caleb P., Dirac Twidwell, Jessica L. Burnett, Victoria M. Donovan, Carissa L. Wonkka,
640 Christine L. Bielski, Ahjond S. Garmestani, et al. 2018. “Early Warnings for State Transitions.”
641 *Rangeland Ecology & Management* 71 (6): 659–70. <https://doi.org/10.1016/j.rama.2018.04.012>.
- 642 Simpson, G. L., and J. Oksanen. 2020. *Analogue Matching and Modern Analogue Technique*
643 *Transfer Function Models. Version 0.17-4*.
- 644 Simpson, Gavin L., and H. John B. Birks. 2012. “Statistical Learning in Palaeolimnology.” In
645 *Tracking Environmental Change Using Lake Sediments: Data Handling and Numerical*
646 *Techniques*, edited by H. John B. Birks, André F. Lotter, Steve Juggins, and John P. Smol, 249–
647 327. Developments in Paleoenvironmental Research. Dordrecht: Springer Netherlands.
648 https://doi.org/10.1007/978-94-007-2745-8_9.
- 649 Smerdon, Jason E. 2012. “Climate Models as a Test Bed for Climate Reconstruction Methods:
650 Pseudoproxy Experiments.” *WIREs Climate Change* 3 (1): 63–77.
651 <https://doi.org/10.1002/wcc.149>.
- 652 Sokolovsky, K. V., P. Gavras, A. Karamelas, S. V. Antipin, I. Bellas-Velidis, P. Benni, A. Z.
653 Bonanos, et al. 2017. “Comparative Performance of Selected Variability Detection Techniques in
654 Photometric Time Series.” *Monthly Notices of the Royal Astronomical Society* 464 (1): 274–92.
655 <https://doi.org/10.1093/mnras/stw2262>.
- 656 Spanbauer, Trisha L., Craig R. Allen, David G. Angeler, Tarsha Eason, Sherilyn C. Fritz, Ahjond
657 S. Garmestani, Kirsty L. Nash, and Jeffery R. Stone. 2014. “Prolonged Instability Prior to a
658 Regime Shift.” Edited by John A. D. Aston. *PLoS ONE* 9 (10).
659 <https://doi.org/10.1371/journal.pone.0108936>.



- 660 Spanbauer, Trisha L., Craig R. Allen, David G. Angeler, Tarsha Eason, Sherilyn C. Fritz, Ahjond
661 S. Garmestani, Kirsty L. Nash, Jeffery R. Stone, Craig A. Stow, and Shana M. Sundstrom. 2016.
662 “Body Size Distributions Signal a Regime Shift in a Lake Ecosystem.” *Proceedings of the Royal*
663 *Society B: Biological Sciences* 283 (1833). <https://doi.org/10.1098/rspb.2016.0249>.
- 664 Taranu, Zofia E., Stephen R. Carpenter, Victor Frossard, Jean-Philippe Jenny, Zoë Thomas,
665 Jesse C. Vermaire, and Marie-Elodie Perga. 2018. “Can We Detect Ecosystem Critical
666 Transitions and Signals of Changing Resilience from Paleo-Ecological Records?” *Ecosphere* 9
667 (10). <https://doi.org/10.1002/ecs2.2438>.
- 668 Telford, R.J., Heegaard, E., Birks, H.J.B., 2004. All Age-Depth Models Are Wrong: But How
669 Badly? *Quaternary Science Reviews* 23, 1–5.
670 <https://doi.org/10.1016/J.QUASCIREV.2003.11.003>
- 671 Williams, John W., Jessica L. Blois, and Bryan N. Shuman. 2011. “Extrinsic and Intrinsic
672 Forcing of Abrupt Ecological Change: Case Studies from the Late Quaternary.” *Journal of*
673 *Ecology* 99 (3): 664–77. <https://doi.org/10.1111/j.1365-2745.2011.01810.x>.
- 674 Zurell, Damaris, Uta Berger, Juliano S. Cabral, Florian Jeltsch, Christine N. Meynard, Tamara
675 Münkemüller, Nana Nehrbass, et al. 2010. “The Virtual Ecologist Approach: Simulating Data
676 and Observers.” *Oikos* 119 (4): 622–35. <https://doi.org/10.1111/j.1600-0706.2009.18284.x>.